A New Ranging Method for OFDMA Systems

Xiaoyu Fu, *Student Member, IEEE*, Yinghui Li, *Student Member, IEEE*, and Hlaing Minn, *Member, IEEE*

***Abstract*— We present a new initial ranging method for OFDMA systems such as IEEE 802.16-2004. First, a new orthogonal ranging signal design is proposed by which an efficient, low-complexity multi-user ranging signal detection is developed. Based on the ranging signal detector results, power estimation for the detected ranging subscriber stations is performed. Then, by utilizing the proposed orthogonal ranging signal design together with the redundancy introduced by cyclic prefixes, a new iterative multi-user timing offset estimator is presented. Compared with the existing methods utilizing the CDMA-type ranging codes (in frequency-domain) defined in IEEE 802.16-2004, the proposed method achieves a better performance and greater robustness against multi-user interference and multi-path fading channels.**

***Index Terms*— OFDMA, ranging process, multi-user ranging code detection, timing estimation, power estimation.**

I. Introduction

ORTHOGONAL frequency division multiple access (OFDMA) has recently received significant interest and has been adopted as one of the three physical layer modes in the IEEE wireless MAN standard 802.16-2004 [1]. In OFDMA, the active sub-carriers are divided into subsets of sub-carriers termed as sub-channels which are assigned to multiple users for simultaneous transmissions. The sub-carriers of each sub-channel may not necessarily be adjacent. To maintain the orthogonality among the sub-carriers in the uplink of OFDMA systems, the signals from all active users should arrive at the base station (BS) synchronously. This is accomplished by an initial uplink synchronization called a ranging process by which ranging subscriber stations (RSSs) adjust their transmission time instants and transmitted powers so that at the BS their ranging signals synchronize to the mini-slot boundary of the BS and have equal power. By means of the ranging process, the system compensates for the near/far problems (different propagation delays, received powers) in large cells. Generally, a ranging process includes initial ranging and periodic ranging. Initial ranging shall be used by any RSS that wants to synchronize to the system for the first time. To account for the user-movement over time, periodic ranging is used. This paper considers initial ranging process.

The basic procedure of initial ranging processing mentioned in IEEE 802.16-2004 [1] is briefly described in the following. First of all, the RSS acquires downlink synchronization and uplink transmission parameters (e.g., ranging channel[1]) from downlink control frames. Then, it shall transmit a randomly chosen frequency-domain ranging code on the ranging channel in a randomly chosen ranging time-slot (one or several OFDM symbols duration). Since more than one RSSs may choose the same time-slot, the received ranging signal may include several RSSs' ranging information. After detecting ranging codes and extracting information of timing and power from the received ranging signal, the BS will broadcast a ranging response message that advertises all the detected ranging codes and corresponding ranging time-slots. The ranging response message also contains adjustment information (e.g., timing and power adjustment) and status notification (e.g., success, re-transmission) corresponding to each detected ranging code. If an RSS receives the success notification, its ranging process is complete. Otherwise, each RSS adjusts its transmission power and timing according to the adjustment information corresponding to its transmitted ranging code, and then repeats its ranging process until success notification. Based on the above procedure, the main tasks of the ranging process at the BS are multi-user ranging code detection, multi-user timing estimation, and power estimation.

In the literature, there are only a few existing works [2]-[4] on the initial ranging process of OFDMA systems. Note that there exist several synchronization methods (e.g., [5] [6] and references therein) for OFDM systems but they cannot be directly applied to OFDMA ranging process due to different system setups. The existing works for the initial ranging process can be divided into two approaches. The first approach, presented in [2] and [3], uses the ranging signals given in IEEE 802.16-2004 [1] where RSSs transmit randomly chosen CDMA code on all the ranging sub-carriers and hence, the corresponding time-domain signals (ranging signals) are overlapped in the time-domain. The method from [2] which is based on a correlator bank in the frequency-domain detects the multi-user ranging codes by a fixed threshold. However, since multi-user interference depends on the number of RSSs, a fixed detection threshold would not give a robust detection performance. The method from [3] which is based on a time-domain correlator bank uses an adaptive detection threshold and achieves an improved detection performance.

The second approach given in [4] employs a new ranging signal structure which divides all ranging signals into several groups. Ranging signals from different groups do not interfere with each other if perfectly synchronized since they are separable in frequency or time by means of transmitting on different sub-channels and introducing different phase shifts. Ranging signals within each group interfere with each other since different CDMA codes are transmitted on the same

Manuscript received May 15, 2005; revised May 1, 2006; accepted June 18, 2006. The associate editor coordinating the review of this paper and approving it for publication was X. Shen. This work was supported by the Erik Jonsson School Research Excellence Initiative, University of Texas at Dallas, Texas, USA.

The authors are with the Department of Electrical Engineering, University of Texas at Dallas, P.O. Box 830688, EC 33, Richardson, TX 75083-0688, USA (email: {xxf031000, yxl044000, hlaing.minn}@utdallas.edu).

Digital Object Identifier 10.1109/LCOMM.2007.05323.

[1]The ranging channel consists of one or more sub-channels over the first few time slots defined by the BS for the ranging process.

sub-channel with the same phase shift. In this scheme, the number of sub-carriers in each sub-channel has to be equal to the length of the CDMA code and the sub-carriers must be assigned adjacently. Hence, it is not applicable in interleaved OFDMA systems. All of the above methods utilize the CDMA codes' correlation properties to distinguish different RSSs'ranging signals overlapped in both time and frequency domains. Their common drawback is that the performance degrades substantially with the channel frequency selectivity and the number of RSSs since the correlation properties of the frequency-domain CDMA codes are affected by the channel frequency selectivity resulting in a larger multiuser interference which is amplified by the larger number of RSSs.

In this paper, we present a new ranging signal design and a new ranging method for interleaved OFDMA systems which overcomes the existing methods' drawback. The proposed ranging signal design does not use frequency-domain CDMA codes of the existing methods but utilizes the orthogonality principle and the best channel identification conditions. This design results in robust, high performance, low-complexity multi-user ranging signal detection and power estimation. A new iterative estimation of timing offsets for all ranging subscriber stations is developed based on the proposed orthogonal ranging signal design and the cyclic prefix redundancy. If compared to existing methods using the existing ranging signals, our ranging signal design and ranging method achieve a better performance and a greater robustness against interference from other subscriber stations and multi-path fading channel effects.

The rest of this paper is organized as follows. The system and signal models are described in Section II. Our ranging signal design is presented in Section III and the proposed ranging method is described in Section IV. Simulation results and discussion are given in Section V and the paper is concluded in Section VI.

Notation: We use the following notations: $[i]_M = i \text{ modulo } M$ and $i_M = \lfloor i/M \rfloor$ where $\lfloor\cdot\rfloor$ denotes the floor operation. Hence $i = i_M M + [i]_M$. The superscripts $*$ and H reprresent the conjugate and the Hermitian transpose. $\Re\{\cdot\}$ and $E[\cdot]$ denote the real part and the statistical expectation. $\mathbf{0}_d$ is the all-zero column vector of a length d.

II. System Description and Signal Model

We consider an uplink of an OFDMA system with N sub-carriers in a time-division duplexing setup. During a ranging time-slot of M symbol intervals, the N sub-carriers are grouped into Q_R ranging sub-channels and Q_D data sub-channels. Each ranging sub-channel has γ_R sub-carriers and each data sub-channel has γ_D sub-carriers where $\gamma_R Q_R + \gamma_D Q_D \leq N$. In general, the sub-carrier assignment of data and ranging sub-channels can be adaptive according to the system and channel conditions.

The indices of all the sub-carriers dedicated for the ranging channel and for the data subscriber stations (DSSs) are denoted by the sets J_R and J_D, and those allocated to the i-th RSS and the k-th DSS are denoted by $J_{i,R}$ and $J_{k,D}$, respectively. Each RSS uses q sub-channels where $1 \leq q \leq Q_R$. During the m-th symbol interval of the ranging time-slot, the i-th RSS transmits $\{C_{i,R}^{(m)}(l):\ l = 0,\ \ldots, q\gamma_R - 1\}$ on the sub-carriers defined by $J_{i,R}$ while the k-th DSS transmits $\{C_{k,D}^{(m)}(l):\ l = 0,\ \ldots, N_{k,D} - 1\}$ on the sub-carriers defined by $J_{k,D}$ where $N_{k,D}$ denotes the cardinality of the set $J_{k,D}$ which would be an integer multiple of γ_D.

In sub-carrier domain at the m-th OFDM symbol interval, the length-N ranging code vector for the i-th RSS and the length-N data vector for the k-th DSS are, respectively, denoted by $\boldsymbol{X}_{i,R}^{(m)}$ and $\boldsymbol{X}_{k,D}^{(m)}$. Their corresponding n-th elements ($n \in \{0,\ \ldots, N-1\}$) are given by

$$X_{i,R}^{(m)}(n) = \begin{cases} A_i C_{i,R}^{(m)}(l), & n = J_{i,R}(l), \\ & l = 0, \ldots, q\gamma_R - 1 \\ 0 & \text{otherwise} \end{cases} \tag{1}$$

$$X_{k,D}^{(m)}(n) = \begin{cases} A_{k,D} C_{k,D}^{(m)}(l), & n = J_{k,D}(l), \\ & l = 0, \ldots, N_{k,D} - 1 \\ 0 & \text{otherwise} \end{cases} \tag{2}$$

where $|C_{i,R}^{(m)}(l)| = |C_{k,D}^{(m)}(l)| = 1$, and $\{A_i,\ A_{k,D} > 0\}$ are amplitude factors. Denote the N-point unitary inverse discrete Fourier transform (IDFT) of $\boldsymbol{X}_{i,R}^{(m)}$ and $\boldsymbol{X}_{k,D}^{(m)}$ by $\boldsymbol{x}_{i,R}^{(m)}$ and $\boldsymbol{x}_{k,D}^{(m)}$, respectively. After cyclic prefix (CP) insertion, the time-domain transmitted signal samples of the i-th RSS are denoted by

$$x_{i,R}(n) = \begin{cases} x_{i,R}^{(m)}(l - N_g), & n = m(N + N_g) + l, \\ & l = 0,\ \ldots, N + N_g - 1; \\ & m = 0, \ldots, M - 1 \\ 0, & \text{otherwise} \end{cases} \tag{3}$$

where $\{x_{i,R}^{(m)}(-l):\ l = 1, \ldots, N_g\}$ represent CP samples and hence, $x_{i,R}^{(m)}(-l) = x_{i,R}^{(m)}(N - l)$. Similarly, those of the k-th DSS are denoted by

$$x_{k,D}(n) = \begin{cases} x_{k,D}^{(m)}(l - N_g), & n = m(N + N_g) + l, \\ & l = 0,\ \ldots, N + N_g - 1; \\ & m = 0, 1, \ldots \\ 0, & n < 0. \end{cases} \tag{4}$$

Suppose that there are N_R RSSs and N_D DSSs in the system and the system can support a maximum of N_c simultaneous RSSs (corresponding to N_c ranging opportunities or distinct ranging signals). The N_R RSSs' ranging signal indices are denoted by the set $\mathcal{I}_R$. For simplicity and without loss of generality, we assume that the i-th RSS uses the ranging signal $\{X_{i,R}(k)\}$, and hence $\mathcal{I}_R = \{0, \ldots, N_R - 1\}$ from the possible indices $\{0,\ \ldots,\ N_c - 1\}$. After obtaining the ranging channel information through the control channel (e.g., UL-MAP in [1]), each RSS chooses one of the N_c ranging signals randomly and performs initial ranging process during one ranging time-slot. Since the locations of different SSs are different, the corresponding transmission delays ($d_{i,R}$ for the i-th RSS and $d_{k,D}$ for the k-th DSS) are different. Hence, at the beginning of the ranging process, their relative delays with respect to the BS's time-slot boundary are different. The maximum possible relative delay $d_{\max,\mathrm{R}}$ for an RSS is the round-trip transmission delay for an RSS at the cell boundary. In practice, we can find this maximum relative delay from the knowledge of cell radius. Note that N_g for RSSs should be designed such that $N_g \geq d_{\max,\mathrm{R}} + L$. For DSSs, since initial

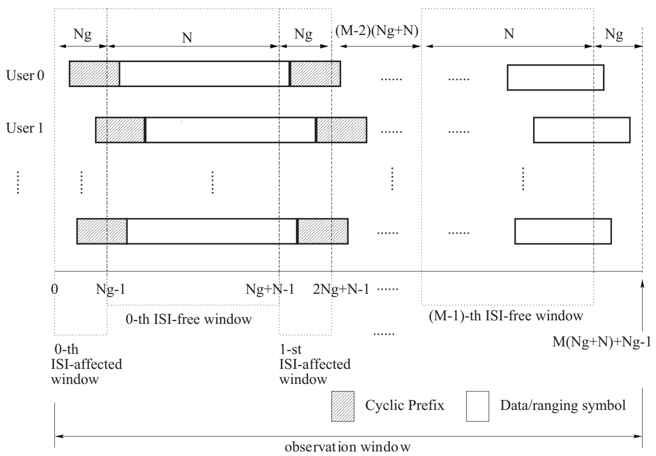

Fig. 1. Observation window at the BS receiver.

ranging processes have already been completed, the maximum possible delay $d_{\max,\mathrm{D}}$, determined by the timing requirement for the ranging process, will be much smaller. Hence, the CP interval for data transmission can be designed to be smaller than that of ranging symbols.

We consider a multi-path Rayleigh fading channel with L sample-spaced taps. The channel tap gains for the i-th RSS and the k-th DSS (denoted by $\{h_{i,R}(l)\}$ and $\{h_{k,D}(l)\}$, $l = 0, \ldots, L-1$, respectively) are assumed to remain constant over one ranging time-slot, and the statistical average total energy of the channel taps is σ_h^2. Let the channel output samples for the i-th RSS signal be $\{y_{i,R}(n)\}$ and those for the k-th DSS be $\{y_{k,D}(n)\}$, i.e.,[2]

$$y_{i,*}(n) = \sum_{l=0}^{L-1} h_{i,*}(l) x_{i,*}(n - l - d_{i,*}). \tag{5}$$

Then the n-th received signal sample ($n = 0, 1, \ldots$) at the BS can be expressed as

$$y(n) = \sum_{i=0}^{N_R-1} y_{i,R}(n) + \sum_{u=0}^{N_D-1} y_{u,D}(n) + w(n) \tag{6}$$

where $\{w(n)\}$ are independent and identically distributed (iid), circularly-symmetric complex Gaussian noise samples with zero mean and variance $\sigma_w^2 = E[|w(n)|^2]$.

At the receiver, we consider an observation window of $M(N + N_g) + N_g$ samples as shown in Fig. 1 to make sure that all received ranging signals reside within this observation window regardless of their possibly different transmission delays. There are M inter-symbol interference (ISI) free windows of N samples each and $(M+1)$ ISI-affected windows of N_g samples each, in the observation window. The sample indices of the m-th ISI-free window and the m-th ISI-affected window are, respectively, denoted by

$$J_{\mathrm{ISI-free}}^{(m)} = \{m(N + N_g) + N_g, \ldots, (m+1)(N + N_g) - 1\},$$
$$m = 0, \ldots, M-1 \tag{7}$$

$$J_{\mathrm{ISI}}^{(m)} = \{m(N + N_g), \ldots, m(N + N_g) + N_g - 1\}$$
$$m = 0, \ldots, M. \tag{8}$$

[2]In the rest of the paper, the subscript * denotes whether R or D.

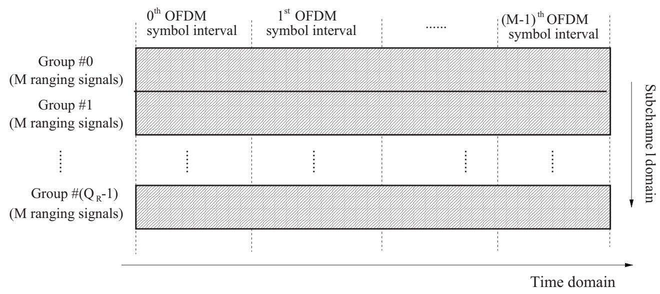

Fig. 2. Ranging opportunities in the subchannel-domain and the time-domain. (Each ranging sub-channel contains disjoint cyclically equal spaced γ_R sub-carriers spread out across the entire bandwidth.)

III. Proposed Ranging Signal Design

We consider an interleaved OFDMA system where $\gamma_R (\geq L)$ sub-carriers of each (initial) ranging sub-channel are spread out across the sub-carrier domain with a cyclically equal spacing of N/γ_R sub-carriers. Each RSS uses γ_R sub-carriers (i.e., $q = 1$). The total number of ranging opportunities (distinct ranging signals) provided by our design is $N_c = Q_R M$ and is shown in Fig. 2.

The N_c different ranging signals are divided into Q_R groups. The signals from different groups are transmitted on different sub-carriers. The sub-carrier assignment for the i-th RSS is defined by

$$J_{i,R} = \{(\frac{nN}{\gamma_R} + \Delta_{i_M}) : \ n = 0, \ldots, \gamma_R - 1\} \tag{9}$$

where

$$0 \leq \Delta_{i_M} < \frac{N}{\gamma_R} \ \& \ \Delta_{i_M} \neq \Delta_{k_M} \text{if } i_M \neq k_M. \tag{10}$$

A recommended choice for Δ_{i_M} is $i_M N/(Q_R \gamma_R)$ which assigns ranging sub-carriers of different groups equally spread out with equal spacing across the entire bandwidth. Note that $\{J_{i,R}\}$ and $\{J_{k,D}\}$ should be disjoint for all i and k and $\{J_{i,R}\}$ and $\{J_{k,R}\}$ are disjoint for all $i_M \neq k_M$ but they are the same if $i_M = k_M$. Due to the orthogonality among sub-carriers, received signals from different groups would not interfere with each other if perfectly frequency-synchronized. On the other hand, the M ranging signals in the same group are transmitted on the same γ_R sub-carriers over M symbol intervals. In order to separate these M ranging signals, we introduce phase-shift-orthogonality over M symbol intervals within each group as follows. The ranging sub-carrier symbols for the i-th RSS at the m-th symbol interval and the 0-th symbol interval are related by

$$C_{i,R}^{(m)}(l) = C_{i,R}^{(0)}(l) e^{j2\pi [i]_M m/M}, \ m = 1, \ldots, M-1. \tag{11}$$

It can be easily observed that all ranging codes are orthogonal to each other, i.e.,

$$\sum_{m=0}^{M-1} \sum_{n=0}^{N-1} X_{i,R}^{(m)}(n) (X_{k,R}^{(m)}(n))^* = \begin{cases} |A_i|^2 \gamma_R M \ , & \text{if } i = k \\ 0 \ , & \text{if } i \neq k. \end{cases} \tag{12}$$

The orthogonality is obtained by either the disjoint sub-carrier assignment as defined in (9) or the phase-shift orthogonality over M symbol intervals as described in (11).

At the receiver under perfectly frequency-synchronized scenario, different ranging codes transmitted on disjoint sub-carriers remain disjoint at the receiver. The orthogonality among different ranging codes transmitted on the same sub-carriers is also maintained at the receiver since the orthogonality is established sub-carrier-wise as described in (11) and the channel gain on each sub-carrier remains the same over the M symbol intervals. Hence, our proposed design provides orthogonality between any signal pairs of the *received* ranging and/or data signals, and hence it is optimal for multi-user ranging code detection if perfectly frequency-synchronized. To elaborate this, first recall that there is no ISI after the CP removal since $N_g \geq d_{\max,R} + L$. Next, there is no multiuser interference in the ranging code detection for the proposed design under perfectly frequency synchronized scenario as shown in (12), and hence an optimal detector (e.g., based on the maximum likelihood criterion) can be derived. However, for the existing ranging codes, there exists multi-user interference in the ranging code detection due to the effect of the channel frequency selectivity on the correlation properties of the received frequency-domain CDMA ranging codes. In this case, the optimal detector cannot be obtained. A benefit of our orthogonal design is that all ranging codes can be easily decoupled, hence rendering an efficient, low-complexity multi-user ranging code detection as will be discussed in the next section.

Note that we set $\gamma_R \geq L$ in our design so that the received ranging signal from any RSS completely characterizes the corresponding channel [3]. Our sub-carrier assignment for ranging sub-channel applies the principle of pilot tone design for MIMO OFDM channel estimation from [11] but we tailor it to the ranging process. Hence, our ranging code design is optimal in terms of characterizing the corresponding channels (may be useful in adaptive resource allocation) which in turn gives a better representation of average power across the sub-carrier domain for the RSS. Note that the existing ranging codes may not be able to provide a complete channel estimate let alone the optimality of the channel estimation. For example, we cannot obtain the channel estimates across all sub-carriers from a ranging code transmitted on a group of adjacent sub-carriers as used in the existing ranging code design from [4].

IV. Proposed Ranging Method

We assume that the ranging signals transmitted by different RSSs in one time-slot are different. By a proper system design, it can be satisfied most of the time. The conflict of more than one RSS using the same ranging signal may be handled by several ways. A simple approach is to embed some subscriber identification information in the ranging signal (for example, designing the ranging time-slot consisting of $M+1$ symbols where the last symbol contains identification information of all RSSs) by which collided RSSs can be distinguished. However, we will not consider this RSS collision issue in this paper. All RSSs first perform frequency synchronization using an appropriate method (e.g., [7]-[9]) based on downlink control/broadcast channel before initiating the ranging process. During the ranging process, residual frequency offset errors will be quite small. Hence, our proposed methods will be developed based on a perfectly frequency-synchronized scenario or a small residual frequency offset scenario. The performance in the presence of residual frequency offsets will be evaluated in the simulation section. Our proposed method first performs multi-user ranging signal detection based on the BS timing reference. Then utilizing the ranging signal detection results, our method carries out power estimation and iterative timing estimation for each detected RSS. Power and timing estimates are compared with ranging requirements and necessary control information is broadcast back to the RSSs.

[3] At least L pilot tones are necessary for the identification of an L-tap channel.

A. Multi-User Ranging Signal Detection

Based on the BS timing reference, we obtain frequency-domain received k-th sub-carrier symbol ($k \in \{0, \ldots, N-1\}$) at the m-th symbol interval ($m \in \{0, \ldots, M-1\}$) by N-point unitary DFT of $\{y(n) : \ n \in J^{(m)}_{\text{ISI-free}}\}$ as

$$\begin{aligned} Y^{(m)}(k) &= \frac{1}{\sqrt{N}} \sum_{l=0}^{N-1} y(m(N+N_g)+N_g+l)e^{-j2\pi lk/N} \\ &= \sum_{i=0}^{N_R-1} X^{(m)}_{i,R}(k) H_{i,R}(k) \\ &+ \sum_{u=0}^{N_D-1} X^{(m)}_{u,D}(k) H_{u,D}(k) + W^{(m)}(k) \end{aligned} \tag{13}$$

where

$$H_{i,R}(k) = e^{\frac{-j2\pi k d_{i,R}}{N}} \sum_{l=0}^{L-1} h_{i,R}(l)\ e^{\frac{-j2\pi lk}{N}} \tag{14}$$

$$H_{i,D}(k) = e^{\frac{-j2\pi k d_{i,D}}{N}} \sum_{l=0}^{L-1} h_{i,D}(l)\ e^{\frac{-j2\pi lk}{N}} \tag{15}$$

$$W^{(m)}(k) = \frac{1}{\sqrt{N}} \sum_{l=0}^{N-1} w(m(N+N_g)+N_g+l)\ e^{\frac{-j2\pi lk}{N}}. \tag{16}$$

Ranging codes using different ranging sub-carriers are already decoupled in the frequency-domain. Within each group of ranging codes using the same ranging sub-carriers, the sub-carrier symbols of different ranging codes can easily be decoupled by utilizing the orthogonality property (see (12), (1) and (11)) as

$$Z_i(k) = \frac{1}{M} \sum_{m=0}^{M-1} Y^{(m)}(k) e^{-j2\pi[i]_M m/M},\ k \in J_{i,R} \tag{17}$$

$$= \begin{cases} X^{(0)}_{i,R}(k) H_{i,R}(k) + \bar{W}(k), & i \in \{0, \ldots, N_R-1\} \\ \bar{W}(k) & i \in \{N_R, \ldots, N_c-1\} \end{cases} \tag{18}$$

where $\{\bar{W}(k)\}$ are iid circularly symmetric complex Gaussian random variables with zero mean and variance σ_w^2/M.

The decision variable D_i to decide the presence of the i-th ranging signal is defined as

$$D_i = \sum_{k\in J_{i,R}} Z_i(k)Z_i^*(k) \tag{19}$$

$$= \begin{cases} \sum_{k\in J_{i,R}} \|X_{i,R}^0(k)H_{i,R}(k)+\bar{W}(k)\|^2, & i\in\mathcal{I}_R \\ \sum_{k\in J_{i,R}} \|\bar{W}(k)\|^2, & i\notin\mathcal{I}_R. \end{cases} \tag{20}$$

The decision variable D_i is not affected by other RSSs and DSSs, resulting in an efficient, low-complexity multi-user ranging signal detection. Our orthogonal ranging signal design is the key to this efficient multi-user ranging signal detection.

The i-th ranging signal detector decides that the i-th ranging signal is detected if $D_i > \eta_i$. The value of the threshold η_i is derived in the following. Since $H_{i,R}(k)$ for $k \in J_{i,R}$ are spread out across the whole bandwidth with equal spacing and $N \gg \gamma_R$ in typical OFDMA systems, $\{H_{i,R}(k): \ k\in J_{i,R}\}$ can be approximately treated as independent random variables. Then D_i is a summation of squares of $2\gamma_R$ approximately iid real-valued Gaussian random variables and can be considered as a chi-square random variable with $2\gamma_R$ degrees of freedom. Hence, the probability density function of D_i can be given by

$$p_{D_i}(x) \approx \frac{1}{\sigma_i^{2\gamma_R}2^{\gamma_R}\Gamma(\gamma_R)}x^{\gamma_R-1}e^{\frac{-x}{2\sigma_i^2}}, x\geq 0 \tag{21}$$

where

$$\sigma_i^2 = \begin{cases} \frac{A_i^2\sigma_h^2}{2}+\frac{\sigma_w^2}{2M}, & i\in\mathcal{I}_R \\ \frac{\sigma_w^2}{2M}, & \text{otherwise.} \end{cases} \tag{22}$$

The detection threshold η_i is derived from the following maximum-likelihood criterion

$$p_{D_{i|i\in\mathcal{I}_R}} \gtrless p_{D_{i|i\notin\mathcal{I}_R}} \tag{23}$$

and obtained as

$$\eta_i = \frac{2\gamma_R\sigma^2_{i|i\notin\mathcal{I}_R}\ \ln\left(\frac{\sigma^2_{i|i\in\mathcal{I}_R}}{\sigma^2_{i|i\notin\mathcal{I}_R}}\right)}{1-\frac{\sigma^2_{i|i\notin\mathcal{I}_R}}{\sigma^2_{i|i\in\mathcal{I}_R}}} \tag{24}$$

$$= \frac{\gamma_R\sigma_w^2}{M}(1+\frac{\gamma_R}{\text{SNR}_iNM})\ln\left(1+\frac{\text{SNR}_iNM}{\gamma_R}\right) \tag{25}$$

where SNR_i is the SNR of the i-th ranging signal defined as

$$\text{SNR}_i = \frac{\gamma_R A_i^2 E[|H_{i,R}(k)|^2]}{N\sigma_w^2} \approx \frac{\gamma_R A_i^2\sigma_h^2}{N\sigma_w^2}. \tag{26}$$

Note that η_i is the same for all i if transmit-powers of all RSSs are the same. Also, under fixed system parameters (γ_R, N, M, σ_w^2), the changes in η_i value due to different SNR values (say within [-10dB $\sim$ 20dB]) is very small and can be neglected when compared with the mean of D_i in the first case ($i\in\mathcal{I}_R$) of (20). So we can use a fixed detection threshold as

$$\eta_i = \frac{\gamma_R\sigma_w^2}{M}\left((1+\frac{\gamma_R}{\text{SNR}_fNM}\right)\ \ln\left(1+\frac{\text{SNR}_fNM}{\gamma_R}\right) \tag{27}$$

where SNR_f is a fixed design SNR for the detection threshold and in our simulation we use $\text{SNR}_f = 100$. To estimate the noise power σ_w^2 required in the detection threshold, we can keep one fixed ranging opportunity (say the i_0-th ranging code) unused. Then D_{i_0} corresponds to the second case ($i \notin \mathcal{I}_R$) of (20) from which the BS receiver can easily estimate the noise power as

$$\hat{\sigma_w^2} = D_{i_0}M/\gamma_R. \tag{28}$$

It is also possible to pre-measure the noise power by other means at the BS without sacrificing a ranging opportunity. We can alternatively use a fixed design value of σ_w^2 for the detection threshold. For environments with varying noise and interference levels, noise (interference included) power estimator could be used, otherwise, a fixed design value of σ_w^2 would be a preferred choice.

In the presence of residual frequency offsets, the σ_i^2 required in the detection threshold can be approximated as (29) (see Appendix-A for details) where v is the design value of the residual normalized (by the sub-carrier spacing) frequency offset. The detection threshold in the presence of residual frequency offset can be calculated from (24) where σ_i^2 is given by (29) and v can be set to the upper end of the possible residual normalized frequency offset range.

B. Power Estimation

After the i-th ranging signal is detected, the next step in the ranging process is to estimate the corresponding (normalized) received power P_i defined by

$$P_i = \frac{\sum_{k\in J_{i,R}} |X_{i,R}(k)|^2|H_{i,R}(k)|^2}{N}. \tag{30}$$

From (20), we obtain

$$P_i = \frac{1}{N}\{D_i - \sum_{k\in J_{i,R}} |\bar{W}_i(n)|^2 - \sum_{k\in J_{i,R}} 2\Re[X_{i,R}(k)H_{i,R}(k)\bar{W}_i(k)]\}. \tag{31}$$

Since the last term in the nominator has a zero mean, we simply estimate the received power of the i-th ranging signal as

$$\hat{P}_i = \frac{D_i - \sigma_w^2\gamma_R/M}{N}. \tag{32}$$

C. Iterative Timing Offset Estimation

The received samples $\{y(n)\}$ are the superposition of signals from N_R RSSs and N_D DSSs with different channels and different timing offsets. Ranging process estimates the timing offsets of all detected RSSs based on the received samples $\{y(n)\}$ within the observation window. We address this multi-user timing offset estimation by means of N_R single RSS timing offset estimators. For each detected RSS, an iterative timing offset estimator is developed. Although multi-user timing offsets are not jointly estimated, each timing offset estimator utilizes the timing offset estimates of the other RSSs obtained in the previous iteration.

The proposed timing offset estimator exploits the proposed orthogonal ranging signal design and the signal redundancy introduced by the CPs. Based on the orthogonality among the RSSs and DSSs signals over M ISI-free windows, we can obtain interference-free clean samples (denoted by $\{\bar{y}_{i,*}^{(m)}(n):$

$$\sigma_i^2 \approx \begin{cases} \left|\frac{1-e^{j2\pi v}}{N(1-e^{j2\pi v/N})}\right|^2 \left[\frac{\sigma_h^2}{2M^2}\sum_{l=0}^{M-1} A_l^2 \left|\frac{1-e^{j2\pi(M(N+N_g)v/N+[l]_M-[i]_M)}}{1-e^{j2\pi[(N+N_g)v/N+([l]_M-[i]_M)/M]}}\right|^2 + \sigma_w^2/(2M)\right], & i \in \mathcal{I}_R \\ \left|\frac{1-e^{j2\pi v}}{N(1-e^{j2\pi v/N})}\right|^2 \left[\frac{\sigma_h^2}{2M^2}\sum_{l=0,l\neq i}^{M-1} A_l^2 \left|\frac{1-e^{j2\pi(M(N+N_g)v/N+[l]_M-[i]_M)}}{1-e^{j2\pi[(N+N_g)v/N+([l]_M-[i]_M)/M]}}\right|^2 + \sigma_w^2/(2M)\right], & \text{otherwise} \end{cases} \tag{29}$$

$n = 0, \ldots, N-1\}$) of the channel-output m-th symbol (except noise contamination) for the i-th SS as (see (18) and (11))

$$\bar{y}_{i,R}^{(m)}(n) = \frac{1}{\sqrt{N}} \sum_{k \in J_{i,R}} Z_i(k) e^{\frac{j2\pi nk}{N}} e^{\frac{j2\pi m [i]_M}{M}} \tag{33}$$

$$\bar{y}_{i,D}^{(m)}(n) = \frac{1}{\sqrt{N}} \sum_{u \in J_{i,D}} Y^{(m)}(u) e^{\frac{j2\pi nu}{N}}. \tag{34}$$

From $\{\bar{y}_{i,*}^{(m)}(n)\}$, we reconstruct, for the i-th RSS (or DSS) with transmission delay d, a clean version of the m-th symbol's CP, $\bar{\boldsymbol{y}}_{i,R,\mathrm{CP}}^{(m)}(d)$ (or $\bar{\boldsymbol{y}}_{i,D,\mathrm{CP}}^{(m)}(d)$) given by

$$\bar{\boldsymbol{y}}_{i,*,\mathrm{CP}}^{(m)}(d) = \tag{35}$$
$$\begin{cases} \left[\mathbf{0}_d, \bar{y}_{i,*}^{(0)}(N-N_g+d), \ldots, \bar{y}_{i,*}^{(0)}(N-1)\right]^T, & m = 0 \\ \left[\bar{y}_{i,*}^{(m-1)}(0), \ldots, \bar{y}_{i,*}^{(m-1)}(d-1), \bar{y}_{i,*}^{(m)}(N-N_g+d), \ldots, \bar{y}_{i,*}^{(m)}(N-1)\right]^T, & m \neq 0. \end{cases}$$

On the other hand, we can obtain another version of the CP (interference-affected version denoted by $\hat{\boldsymbol{y}}_{i,R,\mathrm{CP}}^{(m)}$) by subtracting the clean version of CPs of the other SSs from the received CP within the ISI-affected window, $\boldsymbol{y}_{\mathrm{CP}}^{(m)}$, as follows:

$$\hat{\boldsymbol{y}}_{i,R,\mathrm{CP}}^{(m)} = \boldsymbol{y}_{\mathrm{CP}}^{(m)} - \sum_{k \in \mathcal{I}_R, k \neq i} \bar{\boldsymbol{y}}_{k,R,\mathrm{CP}}^{(m)}(d_{k,R}) - \sum_{u=0}^{N_D-1} \bar{\boldsymbol{y}}_{u,D,\mathrm{CP}}^{(m)}(\tau^{(D)}) \tag{36}$$

where $\tau^{(D)}$ is the design parameter to replace the actual transmission delays for all DSSs since no timing offset estimation for DSS is performed. The $\hat{\boldsymbol{y}}_{i,R,\mathrm{CP}}^{(m)}$ contains correct timing information $d_{i,R}$ (embedded in $\boldsymbol{y}_{\mathrm{CP}}^{(m)}$) and hence, the timing offset estimate for the i-th RSS can be obtained by maximizing a sliding correlation metric between the clean version and the interference-affected version as

$$\hat{d}_{i,R} = \underset{0 \le d \le d_{\max,R}}{\arg\max}\ \Re\left\{\sum_{m=0}^{M-1} \left(\bar{\boldsymbol{y}}_{i,R,\mathrm{CP}}^{(m)}(d)\right)^H \hat{\boldsymbol{y}}_{i,R,\mathrm{CP}}^{(m)}\right\}. \tag{37}$$

Constructing $\hat{\boldsymbol{y}}_{i,R,\mathrm{CP}}^{(m)}$ requires the knowledge of $\{d_{k,R} : k \neq i\}$ which are unknown and what the timing offset estimator for the k-th RSS is estimating. However, we can apply an iterative approach where $\{d_{k,R} : k \neq i\}$ are replaced with $\{\hat{d}_{k,R}^{(0)} : k \neq i\} = \tau^{(R)}$ at the beginning of the first iteration to get the i-th RSS's timing offset estimate $\{\hat{d}_{i,R}^{(1)}\}$ at the end of the first iteration. In general, at the θ-th iteration, the interference-affected version $\hat{\boldsymbol{y}}_{i,R,\mathrm{CP}}^{(m,\theta-1)}$ is constructed by using estimates from the previous iteration, $\{\hat{d}_{k,R}^{(\theta-1)} : k \neq i\}$, and hence, the i-th RSS's timing offset estimate at the θ-th iteration is given by

$$\hat{d}_{i,R}^{(\theta)} = \underset{0 \le d \le d_{\max,R}}{\arg\max}\ \Re\left\{\sum_{m=0}^{M-1} \left(\bar{\boldsymbol{y}}_{i,R,\mathrm{CP}}^{(m)}(d)\right)^H \hat{\boldsymbol{y}}_{i,R,\mathrm{CP}}^{(m,\theta-1)}\right\}. \tag{38}$$

In the following, we will discuss the effect of mismatch between $d_{k,R}$ and $\hat{d}_{k,R}^{(\theta)}$ and how to obtain the values of $\tau^{(D)}$ and $\tau^{(R)}$. Let $\boldsymbol{y}_{i,R,\mathrm{CP}}^{(m)}$ represent $\hat{\boldsymbol{y}}_{i,R,\mathrm{CP}}^{(m)}$ obtained with exact timing offsets of all RSSs and DSSs. Then (38) can be expressed as

$$\begin{aligned} \hat{d}_{i,R}^{\theta} &= \underset{0 \le d \le d_{\max,R}}{\arg\max}\ \Re\left\{\sum_{m=0}^{M-1} \left(\bar{\boldsymbol{y}}_{i,R,\mathrm{CP}}^{(m)}(d)\right)^H \left(\boldsymbol{y}_{i,R,\mathrm{CP}}^{(m)} - \boldsymbol{E}_i^{(m,\theta)}\right)\right\} \\ &= \underset{0 \le d \le d_{\max,R}}{\arg\max}\ \Re\left\{\sum_{m=0}^{M-1} \left(\bar{\boldsymbol{y}}_{i,R,\mathrm{CP}}^{(m)}(d)\right)^H \boldsymbol{y}_{i,R,\mathrm{CP}}^{(m)} - \left(\bar{\boldsymbol{y}}_{i,R,\mathrm{CP}}^{(m)}(d)\right)^H \boldsymbol{E}_i^{(m,\theta)}\right\} \end{aligned} \tag{39}$$

where $\boldsymbol{E}_i^{(m,\theta)}$ is the error vector corresponding to the m-th symbol at the θ-th iteration of the i-th RSS timing offset estimator due to the timing offset mismatches and is defined as

$$\begin{aligned} \boldsymbol{E}_i^{(m,\theta)} &= \hat{\boldsymbol{y}}_{i,R,\mathrm{CP}}^{(m,\theta)} - \boldsymbol{y}_{i,R,\mathrm{CP}}^{(m)} \\ &= \sum_{k \in \mathcal{I}_R, k \neq i} \left(\bar{\boldsymbol{y}}_{k,R,\mathrm{CP}}^{(m)}(d_{k,R}) - \bar{\boldsymbol{y}}_{k,R,\mathrm{CP}}^{(m)}(\hat{d}_{k,R}^{(\theta)})\right) \\ &\quad + \sum_{u=0}^{N_D-1} \left(\bar{\boldsymbol{y}}_{u,D,\mathrm{CP}}^{(m)}(d_{u,D}) - \bar{\boldsymbol{y}}_{u,D,\mathrm{CP}}^{(m)}(\tau^{(D)})\right) \\ &\equiv \sum_{k \in \mathcal{I}_R, k \neq i} \boldsymbol{e}_{k,R,\mathrm{CP}}^{(m,\theta)} + \sum_{u=0}^{N_D-1} \boldsymbol{e}_{u,D,\mathrm{CP}}^{(m)} \end{aligned} \tag{40}$$

and the elements of $\boldsymbol{e}_{k,*,\mathrm{CP}}^{(m,\theta)}$ are zero-mean random variables given by

$$e_{k,*,\mathrm{CP}}^{(m,\theta)}(n) = \begin{cases} 0, \\ (n < \min(d_{k,*}, \hat{d}_{k,*}^{(\theta)})) \cup (n \geq \max(d_{k,*}, \hat{d}_{k,*}^{(\theta)})) \\ \bar{y}_{k,*}^{(0)}(N+n-N_g), \\ (d_{k,*} \le n < \hat{d}_{k,*}^{(\theta)}) \cap (m=0) \\ -\bar{y}_{k,*}^{(0)}(N+n-N_g), \\ (\hat{d}_{k,*}^{(\theta)} \le n < d_{k,*}) \cap (m=0) \\ \bar{y}_{k,*}^{(m)}(N+n-N_g) - \bar{y}_{k,*}^{(m-1)}(n), \\ (d_{k,*} \le n < \hat{d}_{k,*}^{(\theta)}) \cap (m \neq 0) \\ \bar{y}_{k,*}^{(m-1)}(n) - \bar{y}_{k,*}^{(m)}(N+n-N_g), \\ (\hat{d}_{k,*}^{(\theta)} \le n < d_{k,*}) \cap (m \neq 0) \end{cases} \tag{41}$$

where for $* = D$, $e_{k,*,\mathrm{CP}}^{(m,\theta)}(n)$ represents $e_{k,D,\mathrm{CP}}^{(m)}(n)$ and $\hat{d}_{k,*}^{(\theta)}$ represents $\tau^{(D)}$. Since the second term in (40) is due to the DSSs and is irrelevant to timing offsets of RSSs, we need to consider only the first term which represents the interference due to timing mismatches of RSSs. The corresponding interference energy can be calculated (see Appendix-B for details) as (42) and (43).

From (43), we can observe that the interference energy due to timing mismatches is proportional to the difference

$$E\left[(\boldsymbol{e}_{k,R,\mathrm{CP}}^{(m,\theta)})^H(\boldsymbol{e}_{k,R,\mathrm{CP}}^{(m,\theta)})\right] = \begin{cases} E\left[\sum_{n=\min(d_{k,R},\hat{d}_{k,R}^{(\theta)})}^{\max(d_{k,R},\hat{d}_{k,R}^{(\theta)})-1} |\bar{y}_{k,R}^{(m)}(N+n-N_g) - \bar{y}_{k,R}^{(m-1)}(n)|^2\right], & (m \neq 0) \\ E\left[\sum_{n=\min(d_{k,R},\hat{d}_{k,R}^{(\theta)})}^{\max(d_{k,R},\hat{d}_{k,R}^{(\theta)})-1} |\bar{y}_{k,R}^{(0)}(n)|^2\right], & (m = 0) \end{cases} \tag{42}$$

$$\approx \begin{cases} |d_{k,R} - \hat{d}_{k,R}^{(\theta)}|\ 2(\mathrm{SNR}_k\sigma_w^2 + \frac{\gamma_R\sigma_w^2}{NM}), & (m \neq 0) \cap ([N_g]_{\gamma_R} \neq 0) \\ |d_{k,R} - \hat{d}_{k,R}^{(\theta)}|\ 2(\mathrm{SNR}_k\sigma_w^2 + \frac{\gamma_R\sigma_w^2}{NM})(1 - \cos 2\pi\{\frac{[k]_M}{M} + \frac{(N_g)\Delta_{k_M}}{N}\}), & (m \neq 0) \cap ([N_g]_{\gamma_R} = 0) \\ |d_{k,R} - \hat{d}_{k,R}^{(\theta)}|\ (\mathrm{SNR}_k\sigma_w^2 + \frac{\gamma_R\sigma_w^2}{NM}), & (m = 0). \end{cases} \tag{43}$$

$|d_{k,R} - \hat{d}_{k,R}^{(\theta)}|$. Hence, the iterative approach would improve the performance since $\hat{d}_i^{(\theta)}$ can be iteratively improved at SNRs of practical interest. The best number of iterations will be investigated in simulation section.

The best initial timing offset value $\tau^\dagger$ which gives the smallest timing-mismatch-interference energy can be obtained by

$$\tau^\dagger = \arg\min_\tau\{\int_0^{\tau_{\max}} |x-\tau|\ p_\tau(x)\ dx\} \tag{44}$$

where $p_\tau(x)$ is the probability density function of the timing offset τ and

$$\tau_{\max} = \begin{cases} d_{\max,R}, & \text{for RSS} \\ d_{\max,D}, & \text{for DSS.} \end{cases} \tag{45}$$

It is reasonable to assume that the distances of SSs to the BS are uniformly distributed. Then the timing offset $d_{k,*}$ is a random variable with a uniform distribution in $(0, \tau_{\max}]$ and the best initial timing offset value is given by

$$\tau^\dagger = \arg\min_\tau\{\int_0^{\tau_{\max}} \frac{|x-\tau|}{\tau_{\max}}\ dx\} = \frac{\tau_{\max}}{2}. \tag{46}$$

Hence, the best initial timing offset estimates used in our timing offset estimator are given by

$$\tau^{(R)} = \frac{d_{\max,R}}{2} \tag{47}$$

$$\tau^{(D)} = \frac{d_{\max,D}}{2}. \tag{48}$$

Note that the above assumption of the timing offset distribution does not affect our proposed method. A different timing offset distribution may just give a different best initial timing offset value to be used in the estimator. But the performance of our proposed method is not sensitive to a different choice of reasonable initial timing offset value.

V. COMPUTATION COMPLEXITY

The proposed ranging method includes three tasks: multi-user ranging code detection, multi-user timing estimation and power estimation. The BS applies multi-user ranging code detection for the total N_c possible ranging codes which needs $\frac{MN}{2}\log_2 N + (M+1)\gamma_R N_c$ complex multiplications and $MN\log_2 N + (M\gamma_R - 1)N_c$ complex additions. For the iterative timing offset estimator with N_θ iterations and $\hat{N}_R$ detected ranging codes, the computation complexities are $(N_g+d_{\max,R})(\hat{N}_R\gamma_R+Q_D M\gamma_D)+N_\theta\hat{N}_R d_{\max,R}MN_g+M-1$ complex multiplications and $(N_g+d_{\max,R})[\hat{N}_R(\gamma_R-1)+(Q_D\gamma_D-N_D)M]+N_\theta\hat{N}_R[MN_g(N_D+\hat{N}_R)+d_{\max,R}(N_g-1)]$ complex additions. The power estimation requires $\hat{N}_R$ complex multiplications and $\hat{N}_R$ complex additions.

VI. SIMULATION RESULTS AND DISCUSSION

A. Simulation Setup

The OFDMA system parameters are selected from [1]. The uplink bandwidth is 3 MHz, the sub-carrier spacing is 1.67 KHz, and $N = 2048$. The ranging channel has 128 sub-carriers over $M = 2$ symbol intervals. For the proposed ranging signal structure, the parameters used are: $\gamma_R = 8$, $q = 1$, $Q_R = 16$, $\Delta_{i_M} = 16\ i_M$, and $N_c = 32$. We use QPSK format for DSS, and set $\{N_{k,D}\}_{k=0}^{N_D} = \gamma_D = 64$ and $Q_D = N_D$. The combined transmit and receive filter is a raised-cosine filter $g_T(t)$ with a roll-off factor of 0.5. The SUI-3 channel model with 3 paths [10] is used and the statistical average total energy of all channel taps σ_h^2 is set to unity. The channel impulse response for the i-th user is given by

$$h_i(l) = \sum_{i=0}^{2}\epsilon_i\ g_T(lT_s - \tau_i - t_0), \quad l = 0, \ldots, L-1 \tag{49}$$

where $\{\epsilon_i\}$ and $\{\tau_i\}$ are the gains and delays of the channel paths, t_0 is a time shift for causality, and $1/T_s$ is N times the sub-carrier spacing. The number of sample-spaced channel taps, L, is set to 7. Channels of different users are assumed to be independent. We consider a cell radius of 5km which gives the maximum transmission delay (round trip) $d_{\max,R} = 34\mu s$ = 102 samples. N_g is set to 128 samples satisfying the condition $d_{\max,R} < N_g - L$.

The timing requirement based on [1] is that all uplink OFDM symbols should arrive at the BS within an accuracy of $\pm 25\%$ of the minimum guard-interval or better. In [1], N_g can be $1/4$, $1/8$, $1/16$, or $1/32$ of N, and hence, the timing offset should be within ± 16 samples. We set $d_{\max,D} = 32$. For comparison, we include the performance of the methods from [2] and [4] which use the (frequency-domain) CDMA ranging codes. For the method from [2], there are $N_c = 32$ pseudo-noise (PN) ranging codes with 106-bit length each and a ranging signal is generated by modulating one of the ranging codes on the sub-carriers of the ranging channel and repeating it over $M = 2$ symbol intervals. The method from [4] uses 8 generalized chirp-like (GCL) codes with 105-bit length each, and for each code, a total of 4 cyclic phase-shifted versions can be introduced. Hence, the total ranging opportunities is $N_c = 4 \times 8 = 32$ which is consistent with the other two

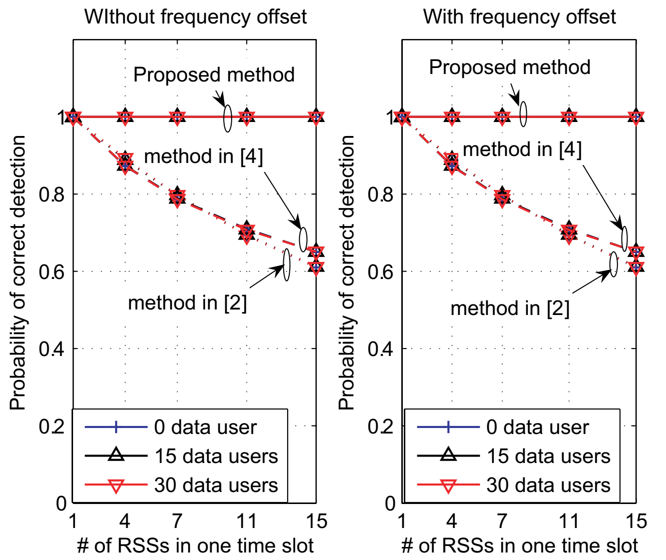

Fig. 3. The probability of correct detection for several ranging code detectors.

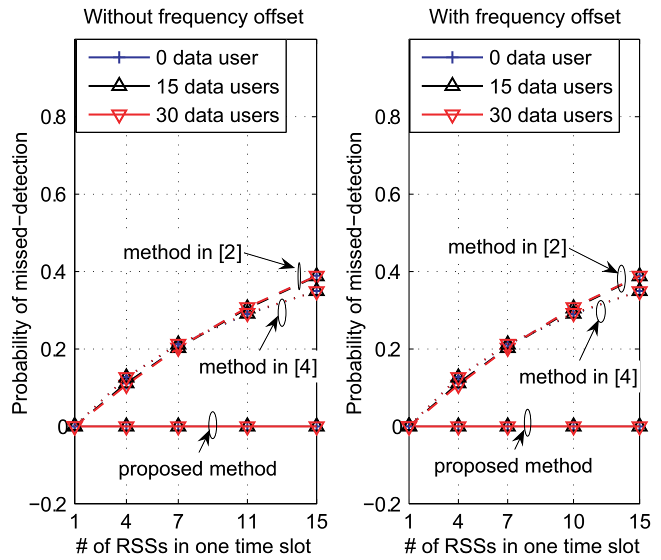

Fig. 5. The probability of missed-detection for several ranging code detectors.

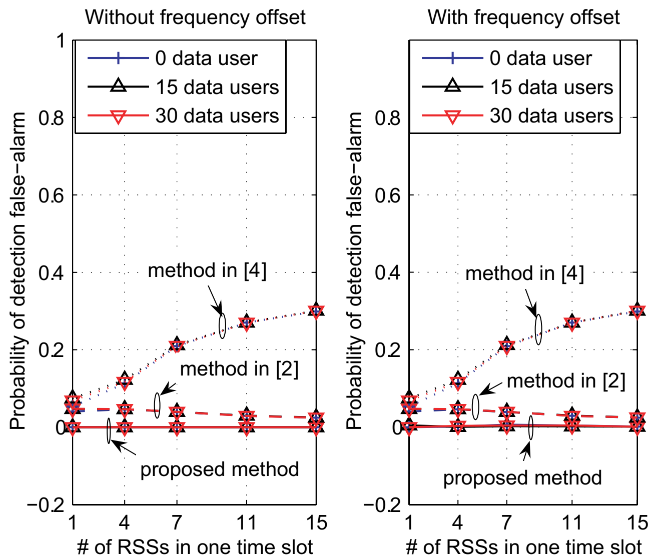

Fig. 4. The probability of detection false-alarm for several ranging code detectors.

methods. In the simulation, the maximum number of RSSs in one time slot, $N_{R,\max}$, is set to 15. We also include residual normalized frequency offsets in the range of $[-0.02,\ 0.02]$ which are assumed to be iid for different SSs. The value of noise power required in setting the detection threshold for the proposed method is obtained by (28).

B. Simulation Results

1) Multi-User Detection Performance : Fig. 3 shows the probability of correct detection ($P_{\rm CD}$) versus the number of RSSs for the conditions of 0 DSS, 15 DSSs, and 30 DSSs in one ranging time-slot. The $P_{\rm CD}$ is defined as $E[\frac{D_c}{N_R}]$ where D_c is the number of correct detection in one ranging time-slot. From Fig. 3, it can be observed that all three methods are robust to the data users' interference and residual frequency offsets. However, the reference methods' $P_{\rm CD}$ performances degrade significantly as the number of RSSs increases (from 1.00 for $N_R = 1$ down to 0.65 for $N_R = 15$) while the proposed method's performance remains the same at $P_{\rm CD} = 1.00$. Hence, the proposed method achieves a better $P_{\rm CD}$ performance over the reference methods.

Fig. 4 shows the probability of detection false-alarm ($P_{\rm FA}$) versus the number of RSSs for the conditions of 0 DSS, 15 DSSs, and 30 DSSs in one ranging time-slot. The $P_{\rm FA}$ is defined as $E[\frac{D_a}{N_c - N_R}]$ where D_a is the number of ranging codes within one ranging time-slot which are detected at the BS but are not transmitted from any RSSs. All methods are robust to frequency offsets. The proposed method and the method from [2] are robust to RSS interference and DSS interference while $P_{\rm FA}$ performance of the method from [4] degrades as the number of RSSs increases. Proposed method has a better $P_{\rm FA}$ performance than both reference methods under all conditions considered.

Fig. 5 shows the probability of missed detection ($P_{\rm MD}$) versus the number of RSSs for the conditions of 0 DSS, 15 DSSs, and 30 DSSs in one ranging time-slot. The $P_{\rm MD}$ is defined as $E[\frac{D_m}{N_R}]$ where D_m is the number of RSSs which are transmitted by RSSs but are not detected at the BS. The proposed method's $P_{\rm MD}$ performance is robust to the DSS interference, RSS interference and frequency offsets while the reference methods' performances degrade as the number of RSSs increases (from $P_{\rm MD} = 0$ at $N_R = 1$ to $P_{\rm MD} = 0.35$ at $N_R = 15$). Hence, the proposed method has a much better performance than both reference methods, especially in multiple RSSs conditions.

2) Power Estimation Performance: Fig. 6 shows the normalized power estimation MSE defined as $E[(1-\frac{\hat{P}_i}{P_i})^2]$ versus the number of RSSs for the conditions of 0 DSS, 15 DSSs, and 30 DSSs in one ranging time-slot. Since there is no power estimator provided in [2] and [4], only the proposed method's performances in the absence/presence of frequency offsets are plotted. Power estimation performance is robust to DSS interference and the number of RSSs in the absence of frequency offsets. We observe that although the power estimation performance degrades as the number of RSSs

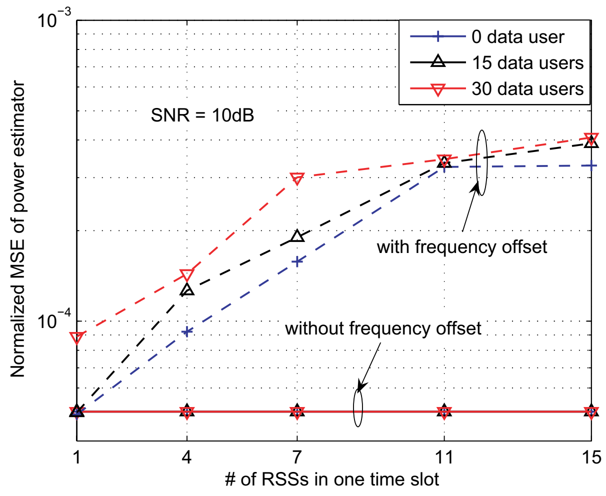

Fig. 6. The normalized MSE of the power estimator at SNR = 10 dB.

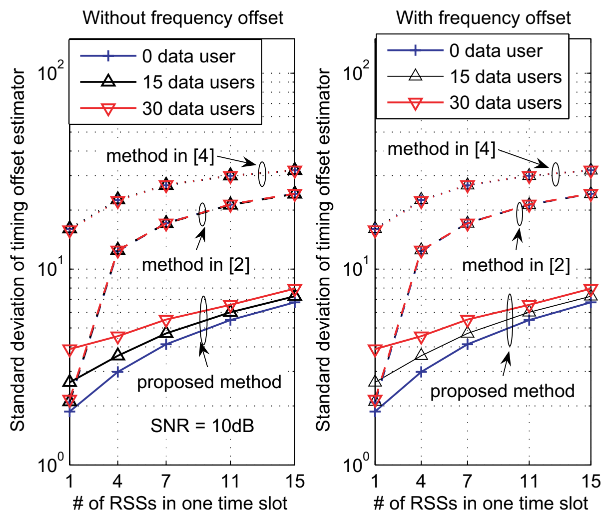

Fig. 7. The standard deviation (in samples) of the timing offset estimators at SNR = 10 dB.

increases in the presence of frequency offsets, the performance is still very good.

3) Timing Estimation Performance: Fig. 7 shows the standard deviation of the timing offset estimate versus the number of RSSs for the conditions of 0 DSS, 15 DSSs, and 30 DSSs in one ranging time-slot. In each simulation run, the true timing offsets for RSSs and DSSs are taken randomly from the interval $[0, d_{\max,\mathrm{R}}]$ and $[0, d_{\max,\mathrm{D}}]$, respectively.

From the figure, it is observed that all the three methods are robust to the DSS interference and residual frequency offsets. The performances of all timing estimators degrade as the numbers of RSSs and DSSs increase but the proposed method gives a much better performance, especially in multiple RSSs condition. Furthermore, the proposed method satisfies the timing requirement defined in [1] all the time while the two reference methods satisfy the requirement only at small RSSs conditions.

Fig. 8 shows the performances of the proposed timing estimator with different numbers of itertions in the presence of frequency offsets. Two iterations would be the best choice since more iterations do not bring in a noticeable improvement.

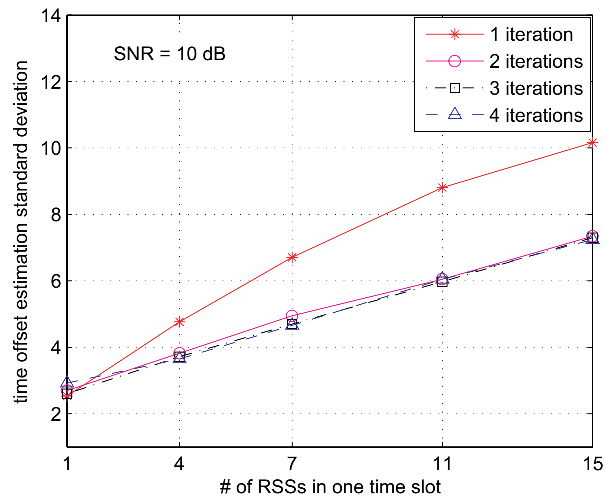

Fig. 8. The performance of the proposed timing offset estimator with different number of iterations (in the presence of frequency offsets and 15 DSSs).

VII. Conclusions

We have presented a new ranging signal design and a new initial ranging method for OFDMA systems in multipath fading channel environments. The proposed ranging signal design is based on the orthogonality principle and the best channel identification conditions. This orthogonal ranging signal design results in robust, high performance, low-complexity multi-user ranging signal detection and power estimation. A new iterative estimation of timing offsets for all ranging subscriber stations is developed based on the proposed orthogonal ranging signal design and the cyclic prefix redundancy. The simulation results show that the new approach is more robust to interference from other ranging/data subscriber stations and multi-path fading channel effects and also has better performance than the existing methods which use the CDMA-type ranging codes in frequency-domain as defined in [2] and [4]. Hence, the proposed approach would be useful in enhancing the IEEE 802.16-2004 standard or developing other OFDMA-based systems.

Appendix-A

In this Appendix, we present detailed steps in obtaining (29) which is used in setting the detection threshold in the presence of residual frequency offsets. Since residual frequency offsets from different users are independent and unknown, in the threshold design, a fixed common design value of residual normalized frequency offset v (upper end of possible residual frequency offset range) will be used. Then the received signal sample at the BS becomes

$$y(n) = e^{\frac{j2\pi n v}{N}} \left(\sum_{i=0}^{N_R-1} y_{i,R}(n) + \sum_{u=0}^{N_D-1} y_{u,D}(n) + w(n) \right). \tag{50}$$

When the i-th ranging code is transmitted by an RSS (i.e., $i \in \mathcal{I}_R$), at the corresponding ranging code detector at the BS, the variable $Z_i(k)$ for $k \in J_{i,R}$ in (17), after decoupling from other users, is given by

$$Z_i(k)=\frac{1}{NM}\sum_{m=0}^{M-1}\sum_{n=0}^{N-1}\Bigg\{\sum_{q\in J_{i,R}}\Bigg(\sum_{l\in\mathcal{I}_R,\ J_{l,R}=J_{i,R}}X_{l,R}^{(m)}(q)H_{l,R}(q)+W^{(m)}(q)\Bigg)e^{\frac{j2\pi qn}{N}}$$
$$+\sum_{a\in\mathcal{I}_R,\ J_{a,R}\neq J_{i,R}}\sum_{l\in J_{a,R}}\left(X_{a,R}^{(m)}(l)H_{a,R}(l)+W^{(m)}(l)\right)e^{\frac{j2\pi ln}{N}}$$
$$+\sum_{u=0}^{N_D-1}\sum_{p\in J_{u,D}}\left(X_{u,D}^{(m)}(p)H_{u,D}(p)+W^{(m)}(p)\right)e^{\frac{j2\pi pn}{N}}\Bigg\}$$
$$\times e^{\frac{j2\pi(m(N+N_g)+N_g+n)v}{N}}e^{\frac{-j2\pi nk}{N}}e^{\frac{-j2\pi m[i]_M}{M}}$$
$$=\frac{1}{N}e^{\frac{j2\pi N_g v}{N}}\Bigg\{\sum_{n=0}^{N-1}\sum_{q\in J_{i,R}}e^{\frac{j2\pi n(q-k+v)}{N}}\Bigg[\sum_{l\in\mathcal{I}_R,\ J_{l,R}=J_{i,R}}$$
$$X_{l,R}^{(0)}(q)H_{l,R}(q)\frac{1}{M}\sum_{m=0}^{M-1}e^{j2\pi m(\frac{(N+N_g)v}{N}+\frac{[l]_M-[i]_M}{M})}$$
$$+\frac{1}{M}\sum_{m=0}^{M-1}W^{(m)}(q)e^{j2\pi m(\frac{(N+N_g)v}{N}-\frac{[i]_M}{M})}\Bigg]$$
$$+\sum_{n=0}^{N-1}\sum_{a\in\mathcal{I}_R,\ J_{a,R}\neq J_{i,R}}\sum_{l\in J_{a,R}}e^{\frac{j2\pi n(l-k+v)}{N}}\Bigg[$$
$$X_{a,R}^{(0)}(l)H_{a,R}(l)\frac{1}{M}\sum_{m=0}^{M-1}e^{j2\pi m(\frac{(N+N_g)v}{N}+\frac{[a]_M-[i]_M}{M})}$$
$$+\frac{1}{M}\sum_{m=0}^{M-1}W^{(m)}(l)e^{j2\pi m(\frac{(N+N_g)v}{N}-\frac{[i]_M}{M})}\Bigg]$$
$$+\sum_{n=0}^{N-1}\sum_{u=0}^{N_D-1}\sum_{p\in J_{u,D}}e^{\frac{j2\pi n(p-k+v)}{N}}\frac{1}{M}\sum_{m=0}^{M-1}$$
$$\left[X_{u,D}^{(m)}(p)H_{u,D}(p)+W^{(m)}(l)\right]e^{j2\pi m(\frac{(N+N_g)v}{N}-\frac{[i]_M}{M})}\Bigg\}$$
$$=\frac{1}{N}e^{\frac{j2\pi N_g v}{N}}\Bigg\{\sum_{q\in J_{i,R}}\Bigg[\sum_{l\in\mathcal{I}_R,\ J_{l,R}=J_{i,R}}X_{l,R}^{(0)}(q)H_{l,R}(q)$$
$$\times\frac{1-e^{j2\pi(M(N+N_g)v/N+[l]_M-[i]_M)}}{M(1-e^{j2\pi[(N+N_g)v/N+([l]_M-[i]_M)/M]})}+\bar{W}(q)\Bigg]$$
$$\times\frac{1-e^{j2\pi(q-k+v)}}{1-e^{j2\pi(q-k+v)/N}}$$
$$+\sum_{a\in\mathcal{I}_R,\ J_{a,R}\neq J_{i,R}}\sum_{l\in J_{a,R}}\Bigg[X_{a,R}^{(0)}(l)H_{i,R}(l)$$
$$\times\frac{1-e^{j2\pi[M(N+N_g)v/N+([a]_M-[i]_M)]}}{M(1-e^{j2\pi[(N+N_g)v/N+([a]_M-[i]_M)/M]})}+\bar{W}(l)\Bigg]$$
$$\times\frac{1-e^{j2\pi(l-k+v)}}{1-e^{j2\pi(l-k+v)/N}}$$
$$+\sum_{u=0}^{N_D-1}\sum_{p\in J_{u,D}}\frac{1}{M}\sum_{m=0}^{M-1}\left[X_{u,D}^{(m)}(p)H_{u,D}(p)+W^{(m)}(l)\right]$$
$$e^{j2\pi m(\frac{(N+N_g)v}{N}-\frac{[i]_M}{M})}\frac{1-e^{j2\pi(u-k+v)}}{1-e^{j2\pi(u-k+v)/N}}\Bigg\}\qquad(51)$$

where $\{\bar{W}(l)\}$ are iid circularly symmetric complex Gaussian random variable with zero mean and variance σ_w^2/M.

Since residual frequency offsets are typically quite small, the inter-carrier interference (ICI) from other users with *different* sub-carriers will be very small and hence can be neglected. In other words, we can consider only the different ranging signals with the *same* ranging sub-carriers. Then for $i\in\mathcal{I}_R$ and $k\in J_{i,R}$, we have

$$Z_i(k)\approx\frac{e^{\frac{j2\pi N_g v}{N}}(1-e^{j2\pi v})}{N(1-e^{j2\pi v/N})}\Bigg[\sum_{l\in\mathcal{I}_R,\ J_{l,R}=J_{i,R}}X_{l,R}^{(0)}(k)H_{l,R}(k)$$
$$\frac{1-e^{j2\pi(M(N+N_g)v/N+[l]_M-[i]_M)}}{M(1-e^{j2\pi[(N+N_g)v/N+([l]_M-[i]_M)/M]})}+\bar{W}(k)\Bigg].\qquad(52)$$

When the i-th ranging code is not transmitted (i.e., $i\notin\mathcal{I}_R$), we have, at the i-th ranging code detector and for $k\in J_{i,R}$,

$$Z_i(k)\approx\frac{1}{NM}\sum_{m=0}^{M-1}\sum_{n=0}^{N-1}\sum_{q\in J_{i,R}}\Bigg[\sum_{l\in\mathcal{I}_R,\ J_{l,R}=J_{i,R}}X_{l,R}^{(m)}(q)H_{l,R}(q)$$
$$+W^{(m)}(q)\Bigg]e^{\frac{j2\pi(m(N+N_g)+N_g+n)v}{N}}e^{\frac{j2\pi n(q-k)}{N}}e^{\frac{-j2\pi m[i]_M}{M}}$$
$$=\Bigg[\sum_{l\in\mathcal{I}_R,\ J_{l,R}=J_{i,R}}X_{l,R}^{(0)}(k)H_{l,R}(k)$$
$$\times\frac{1-e^{j2\pi(M(N+N_g)v/N+[l]_M-[i]_M)}}{M(1-e^{j2\pi[(N+N_g)v/N+([l]_M-[i]_M)/M]})}$$
$$+\bar{W}(k)\Bigg]\frac{e^{\frac{j2\pi N_g v}{N}}(1-e^{j2\pi v})}{N(1-e^{j2\pi v/N})}.\qquad(53)$$

For both cases of $i\in\mathcal{I}_R$ and $i\notin\mathcal{I}_R$, the statistics of $Z_i(k)$ for $k\in J_{i,R}$ depend on how many RSSs have transmitted on the same sub-carriers within the same ranging time-slot. For determining the detection threshold, we can adopt the scenarios where all M ranging signals are present for the case of $i\in\mathcal{I}_R$ and the $(M-1)$ ranging signals other than the i-th ranging signal are present for the case of $i\notin\mathcal{I}_R$. These scenarios represent worst-case interference from the sub-carriers in $J_{i,R}$ and are chosen because we have already neglected interference from DSSs. Under these scenarios, combining (52) and (53) gives (54) for $k\in J_{i,R}$.

Then, similar to the case without frequency offsets, the σ_i^2 required in the detection threshold is straight-forwardly obtained from (54) as given in (29).

APPENDIX-B

This Appendix presents detailed steps in obtaining (43). From (42), we just need to consider the following term

$$E[|\bar{y}_{k,R}^{(m)}(N-N_g+n)-\bar{y}_{k,R}^{(m-1)}(n)|^2]$$
$$=E\left[|\bar{y}_{k,R}^{(m)}(N-N_g+n)|^2\right]+E\left[|\bar{y}_{k,R}^{(m-1)}(n)|^2\right]$$
$$-2\Re\left\{E\left[\bar{y}_{k,R}^{(m)}(N-N_g+n)(\bar{y}_{k,R}^{(m-1)}(n))^*\right]\right\}.\qquad(55)$$

Since $H_{k,R}(l)$ and $H_{k,R}(q)$ for $l\neq q$ are approximately-independent random variables with zero mean, we have

$$E\left[|\bar{y}_{k,R}^{(m)}(n)|^2\right]$$
$$=\frac{1}{N}E\Bigg[\sum_{l\in J_{k,R}}\sum_{q\in J_{k,R}}\left(X_{k,R}^{(0)}(l)H_{k,R}(l)+\bar{W}(l)\right)$$
$$\left(X_{k,R}^{(0)}(q)H_{k,R}(q)+\bar{W}(q))^*\right)\Bigg]e^{\frac{j2\pi n(q-l)}{N}}$$
$$\approx\frac{1}{N}E\Bigg[\sum_{l\in J_{k,R}}\left\{|X_{k,R}^{(0)}(l)|^2|H_{k,R}(l)|^2+|\bar{W}(l)|^2\right\}\Bigg]$$
$$\approx\frac{1}{N}\sum_{l\in J_{k,R}}\left\{A_k^2E\left[|H_{k,R}(l)|^2\right]+\frac{\sigma_w^2}{M}\right\}$$
$$=\frac{\gamma_R A_k^2\sigma_h^2}{N}+\frac{\gamma_R\sigma_w^2}{NM}\approx\mathrm{SNR}_k\ \sigma_w^2+\frac{\gamma_R\sigma_w^2}{NM}\qquad(56)$$

$$Z_i(k) \approx \begin{cases} \frac{e^{\frac{j2\pi N_g v}{N}}(1-e^{j2\pi v})}{N(1-e^{j2\pi v/N})} \left[\sum_{l=0}^{M-1} X_{l,R}^{(0)}(k) H_{l,R}(k) \frac{1-e^{j2\pi(M(N+N_g)v/N+[l]_M-[i]_M)}}{M(1-e^{j2\pi[(N+N_g)v/N+([l]_M-[i]_M)/M]})} + \bar{W}(k) \right], & i \in \mathcal{I}_R \\ \frac{e^{\frac{j2\pi N_g v}{N}}(1-e^{j2\pi v})}{N(1-e^{j2\pi v/N})} \left[\sum_{l=0,\ l\neq i}^{M-1} X_{l,R}^{(0)}(k) H_{l,R}(k) \frac{1-e^{j2\pi(M(N+N_g)v/N+[l]_M-[i]_M)}}{M(1-e^{j2\pi[(N+N_g)v/N+([l]_M-[i]_M)/M]})} + \bar{W}(k) \right], & i \notin \mathcal{I}_R. \end{cases} \quad (54)$$

and

$$\begin{aligned} & E\left[\bar{y}_{k,R}^{(m)}(N-N_g+n)\left(\bar{y}_{k,R}^{(m-1)}(n)\right)^*\right] \\ & = E\left[\frac{1}{N}\left\{\sum_{l\in J_{k,R}}\left(X_{k,R}^{(0)}(l)H_{k,R}(l)+\bar{W}(l)\right)\right.\right. \\ & \left.\times\ e^{-j2\pi(\frac{l(N-N_g+n)}{N}-\frac{[k]_M m}{M})}\right\} \\ & \times\left\{\sum_{q\in J_{k,R}}\left(X_{k,R}^{(0)}(q)H_{k,R}(q)+\bar{W}(q)\right)^* \right. \\ & \left.\left.\times e^{j2\pi(\frac{qn}{N}-\frac{[k]_M(m-1)}{M})}\right\}\right] \\ & \approx \frac{1}{N}e^{\frac{j2\pi[k]_M}{M}}\left\{\sum_{l\in J_{k,R}}\left(E\left[|X_{k,R}^{(0)}(l)H_{k,R}(l)|^2\right]\right.\right. \\ & \left.+\ E\left[|\bar{W}(l)|^2\right]\right)e^{-j2\pi\frac{l(N-N_g)}{N}}\right\} \end{aligned}$$

$$\begin{aligned} & \approx \left(\frac{A_k^2\sigma_h^2}{N}+\frac{\sigma_w^2}{NM}\right)e^{\frac{j2\pi[k]_M}{M}}\sum_{n=0}^{\gamma_R-1}e^{\frac{-j2\pi(N-N_g)(nN+\gamma_R\Delta_{k_M})}{N\gamma_R}} \\ & \approx \left(\frac{A_k^2\sigma_h^2}{N}+\frac{\sigma_w^2}{NM}\right)e^{j2\pi\{\frac{[k]_M}{M}+\frac{N_g\Delta_{k_M}}{N}\}}\sum_{n=0}^{\gamma_R-1}e^{\frac{j2\pi N_g n}{\gamma_R}} \\ & \approx \begin{cases} 0\ , & ([N_g]_{\gamma_R}\neq 0) \\ \left(\frac{A_k^2\sigma_h^2}{N}+\frac{\sigma_w^2}{NM}\right)\gamma_R e^{j2\pi\{\frac{[k]_M}{M}+\frac{N_g\Delta_{k_M}}{N}\}}, & ([N_g]_{\gamma_R}=0). \end{cases} \end{aligned} \quad (57)$$

Substituting (56) and (57) into (55), and then into (42) gives (43).

REFERENCES

[1] IEEE LAN/MAN Standards Committee, "Broadband Wireless Access: IEEE MAN standard," IEEE 802.16-2004, 2003.

[2] J. Krinock, M. Singh, M. Paff, A. Lonkar, L. Fung, and C.-C. Lee, "Comments on OFDMA ranging scheme described in IEEE 802.16ab-01/01r1," document IEEE 802.16abc-01/24.

[3] X. Fu and H. Minn, "Initial uplink synchronization and power control (ranging process) for OFDMA systems," in *Proc. Globecomm 2004*, pp. 3999-4003.

[4] X. Zhuang, K. Baum, V. Nangia, and M. Cudak "Ranging improvement for 802.16e OFDMA PHY," document IEEE 802.16e-04/143r1.

[5] H. Minn, V. K. Bhargava, and K. B. Letaief, "A robust timing and frequency synchronization for OFDM systems," *IEEE Trans. Wireless Commun.*, vol. 2, no. 4, pp. 822-839, July 2003.

[6] H. Minn, V. K. Bhargava, and K. B. Letaief, "A combined timing and frequency synchronization and channel estimation for OFDM," *IEEE Trans. Commun.*, vol. 54, no. 3, pp. 416-422, Mar. 2006.

[7] H. Minn, P. Tarasak, and V. K. Bhargava, "OFDM frequency offset estimation based on BLUE principle," in *Proc. IEEE VTC 2002 (Fall)*, pp. 1230-1234.

[8] H. Minn, P. Tarasak and V. K. Bhargava, "Some issues of complexity and training symbol design for OFM frequency offset estimation methods based on BLUE principle," in *Proc. IEEE VTC 2003 (Spring)*, pp. 1288-1292.

[9] X. Fu and H. Minn, "Modified data-pilot-multiplexed scheme for OFDM systems," in *IEEE VTC 2005 (Fall)*, vol. 2, pp. 1011-1015.

[10] IEEE LAN/MAN Standards Committee, "Channel Models for Fixed Wireless Applications," document IEEE.802.16.3c-01/29r4.

[11] H. Minn and N. Al-Dhahir, "Optimal training signals for MIMO OFDM channel estimation," *IEEE Trans. Wireless Commun.*, vol. 5, no. 5, pp. 1158-1168, May 2006.

[12] IEEE LAN/MAN Standards Committee, "Broadband Wireless Access: IEEE MAN standard," IEEE 802.16, 2004.

Xiaoyu Fu (S'04) received the B.S. and M.S. degree in electrical engineering from the University of Electronic Science and Technology of China, Sichuan, China, in 1999 and 2002, respectively. He is working toward the Ph.D. degree at the University of Texas at Dallas (UTD), Dallas. Since 2003, he has been a research assistant with the Information and Communication Systems Laboratory at the Department of Electrical Engineering, UTD. His research interests include wireless communications and statistic signal processing.

Yinghui Li (S'05) received the B.E. and M.S. degree in electrical engineering from the Nanjing University of Aeronautics and astronautics, Nanjing, China, in 2000 and 2003, respectively. She is currently working toward the Ph.D. degree in electrical engineering at the University of Texas at Dallas. Her research interests are in the applications of statistical signal processing and training signal designs in synchronization, channel estimation and detection problems in broadband wireless communications.

Hlaing Minn (S'99-M'01) received his B.E. degree in electronics from Yangon Institute of Technology, Yangon, Myanmar, in 1995, the M.Eng. degree in telecommunications from the Asian Institute of Technology (AIT), Pathumthani, Thailand, in 1997, and the Ph.D. degree in electrical engineering from the University of Victoria, Victoria, BC, Canada, in 2001.

He was with the Telecommunications Program in AIT as a laboratory supervisor during 1998. He was a research assistant from 1999 to 2001 and a post-doctoral research fellow during 2002 in the Department of Electrical and Computer Engineering at the University of Victoria. Since September 2002 he has been with the Erik Jonsson School of Engineering and Computer Science, the University of Texas at Dallas, USA, as an assistant professor. His research interests include wireless communications, statistical signal processing, error control, detection, estimation, synchronization, signal design, and cross-layer design. He is an editor for the *IEEE Transactions on Communications*.